

An Experimental Study on Natural Convection from Vertical Surfaces Embedded in Porous Media

S. U. Rahman,* M. A. Al-Saleh, and R. N. Sharma

Department of Chemical Engineering, King Fahd University of Petroleum & Minerals, Dhahran 31261, Saudi Arabia

Mass-transfer coefficients for natural convection from vertical surfaces embedded in saturated porous media have been experimentally obtained by utilizing a limiting diffusion current technique based on cathodic reduction of cupric ions in an acidic solution. The data correspond to a high Rayleigh number and exhibit non-Darcian effects. Final results, when compared with available mathematical models, revealed that a model based on Brinkman-extended Darcy's flow model with a corrected constant predicted mass-transfer coefficients closely. For the spherical packing materials the data fit well in, $Sh_L^* = 3.32(Ra_L^*/Da_L)^{0.26}$, where Ra_L^* and Da_L are a modified Rayleigh number and Darcy's number, respectively.

1. Introduction

Natural convection from surfaces embedded in porous media has been receiving constant attention for its importance in several applications such as petroleum reservoir engineering, thermal insulation of buildings and process equipment, storage of heat-generating materials (e.g., grains, some catalysts, coal, etc.), nuclear waste disposal, and geophysical applications. Numerous theoretical and a few experimental investigations have been carried out to study the natural convection from vertical surfaces embedded in saturated porous media.^{1,2} The problem was first addressed by Cheng and Minkowycz.³ They obtained similarity solutions based on Darcy's law and boundary-layer approximations. Cheng and Hsu⁴ and Joshi and Gebhart⁵ examined higher order effects to extend the range of applicability of the boundary-layer analysis based on Darcy's law. A number of studies have considered various non-Darcian effects on the same problem. Bejan and Poulikakos⁶ and Plumb and Huenefeld⁷ used Forschheimer's equation to include inertia effects. Hsu and Cheng⁸ and Evans and Plumb⁹ studied boundary-layer effects based on Brinkman's equation. Kim and Vafai¹⁰ employed the Brinkman-extended Darcy model. Experimental studies in this area are scarce. Evans and Plumb⁹ found good agreement with the Cheng and Minkowycz theory below $Ra_x < 400$. Cheng et al.¹¹ used 3-mm glass beads and observed a reasonable match with the theory for $Ra_x < 300$. Kaviany and Mittal^{12,13} performed experiments with high permeability polyurethane foams saturated with air. Their results matched fairly well with their theory based on the Brinkman–Forschheimer formulation. In all of these experiments, inertial effects were not significant because Rayleigh numbers were not high enough. The objective of the present work is to experimentally obtain natural convective mass-transfer coefficients from vertical surfaces embedded in saturated porous media, utilizing an electrochemical limiting diffusion current technique (LDCT). Rayleigh numbers in this study are high because of a higher Schmidt number of the acidic cupric sulfate solution and therefore exhibit significant non-Darcian effects. The results

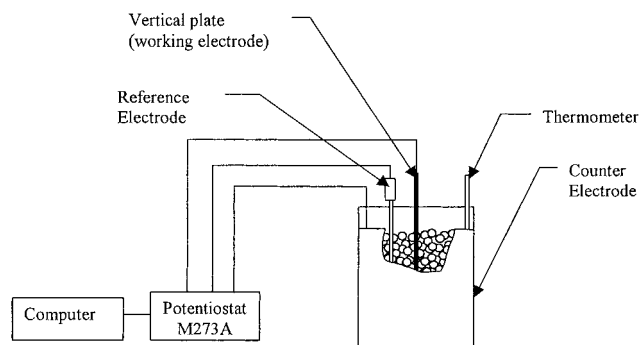


Figure 1. Experimental setup for measuring the limiting current.

are compared with the predictions of available mathematical models for natural heat/mass transfer.

2. Experimental Section

The experimental setup used for the present study is shown in Figure 1. The packed bed was formed in a 1-L cylindrical vessel with five different packing materials, namely, glass spheres of 16, 6, 4, and 3 mm diameter and sand of 0.3 mm average particle diameter. The average diameter of the sand particles was determined by measuring the size of several typical particles. Porosities of the packing materials were determined by a water replacement method. Copper reduction from an acidic cupric sulfate solution was chosen to estimate the limiting diffusion current. This system was selected for its well-defined limiting current plateau.¹⁴ A solution of 0.618 M $CuSO_4$ and 3.09 M H_2SO_4 was prepared. Concentrations of Cu^{2+} and H_2SO_4 were determined through idiometric and acid–base titration, respectively.

Eight copper strips (15.0 cm × 1.1 cm × 0.2 cm) were used as embedded surfaces at which mass-transfer coefficients were sought. The surface was prepared by application of increasing grades of emery papers (100, 400, 600, and 1500 grit size) and finally by washing of with acetone to remove any oil/grease. Samples were masked with insulating paint to expose a predetermined area on each strip. The prepared sample was vertically embedded in the packing material to act as the working electrode. A copper cylinder kept inside the bed, near

* Corresponding author. E-mail: srahman@kfupm.edu.sa.

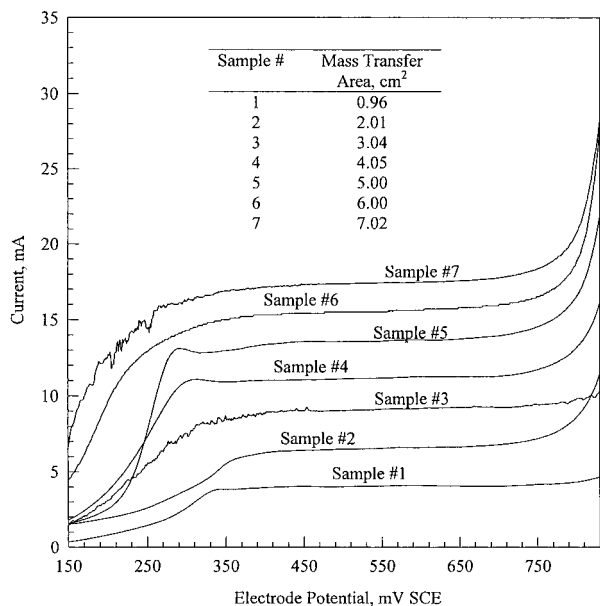


Figure 2. Potentiostatic polarization curves showing limiting currents for vertical copper plates in a CuSO_4 solution.

the wall, worked as the counter electrode. A saturated calomel electrode was embedded in the bed to function as a reference electrode. The temperature of the solution was measured by a thermometer of 0.1 °C least count. The working, counter, and reference electrodes were connected to a potentiostat (model 273A, EG&G PARC). The potentiostat was driven by software (model 352, EG &G PARC) via an IBM486 computer. Potentiostatic linear polarization curves were obtained for all sample strips embedded in different packing materials.

3. Data Reduction

Typical polarization curves obtained for a vertical surface in a free solution are shown in Figure 2. Similar curves were obtained when the surface was embedded in porous media. These curves exhibit a pronounced limiting current plateau between 450 and 650 mV SCE. The limiting current determined from these curves is used to calculate the average mass-transfer coefficients (k_L):

$$k_L = \frac{I_L}{zFAC_b} \quad (1)$$

The physicochemical properties of the acidic cupric sulfate solution, which are required to calculate Sherwood and Rayleigh numbers, were estimated from a temperature-dependent empirical correlation given in the Appendix. The density of the solution at the surface (ρ_0) is also needed to evaluate the Rayleigh number. Its evaluation necessitates estimation of concentration of H_2SO_4 and CuSO_4 at the surface. For a mass-transfer-controlled regime, the surface concentration of CuSO_4 can be taken as zero while the concentration of H_2SO_4 is calculated by utilizing the principle of electroneutrality and the correlation given in ref 15.

The effective mass diffusivity for a given media is estimated from the molecular diffusivity by the following relation:¹⁶

$$D_e = D\epsilon/\tau \quad (2)$$

Table 1. Range of Various Parameters in This Study

parameter	range
particle diameter (mm)	0.3–16.0
temperature (°C)	20.9–23.8
porosity	0.371–0.417
permeability (cm ²)	1.03×10^{-6} – 3.38×10^{-3}
Sc	3910–4460
Ra	2.0×10^8 – 1.4×10^{11}
Ra^*	2.0×10^3 – 6.9×10^7

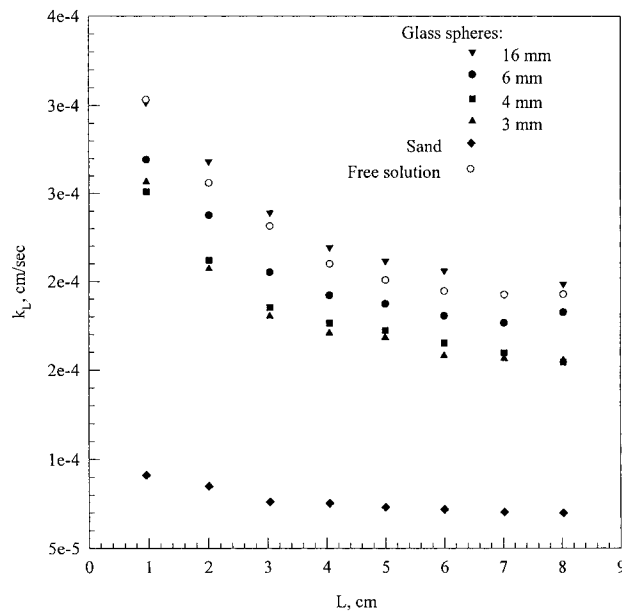


Figure 3. Average mass-transfer coefficients for vertical surfaces embedded in different packing materials.

where τ is the tortuosity of the porous media. For regular packing materials, its recommended value¹⁶ is 4. The permeability of the media is estimated using Carman-Kozeny's equation:²

$$K = \frac{d_p^2 \epsilon}{180(1 - \epsilon)^2} \quad (3)$$

4. Results and Discussion

Table 1 shows the range of various parameters used in the experiments.

The average mass-transfer coefficients estimated by eq 1 are plotted against embedded lengths for different packing materials and a free solution in Figure 3. The mass-transfer coefficients decrease with length, conforming to the inferences of the boundary-layer theory. In general, the mass-transfer coefficient increases with the particle size of the packing, asymptotically approaching the values for the free solution except for 16 mm glass spheres. Because the data have been taken at different temperatures, the dependency of the mass-transfer coefficient on packing material cannot be established on the basis of k_L vs L curves without nondimensionalization. In Figure 4 mass-transfer data are plotted as Sh_L versus $Ra_L^{0.25}$ for all situations. Most of the data are in the laminar range except toward the higher side of Ra_L . The experimental data for the free solution match the equation developed through laminar boundary-layer analysis:¹⁷

$$Sh_L = 0.677 Ra^{0.25} \left[\frac{0.952}{Sc} + 1 \right]^{-0.25} \quad (4)$$

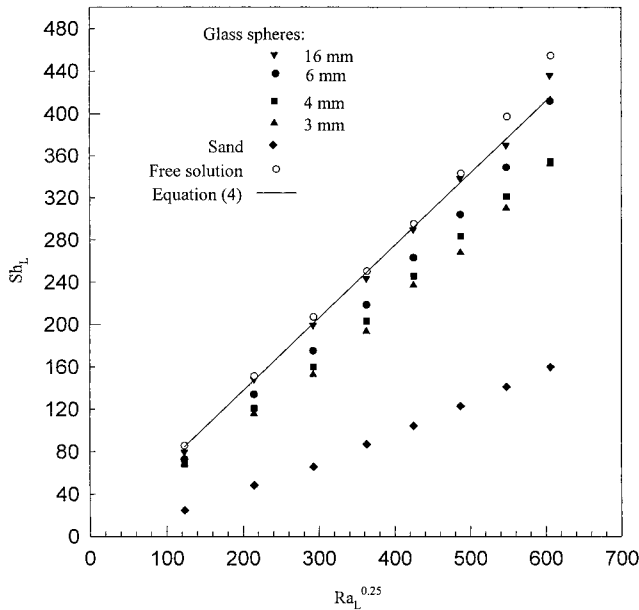


Figure 4. Variation of the average Sherwood number with Rayleigh numbers for different packing materials.

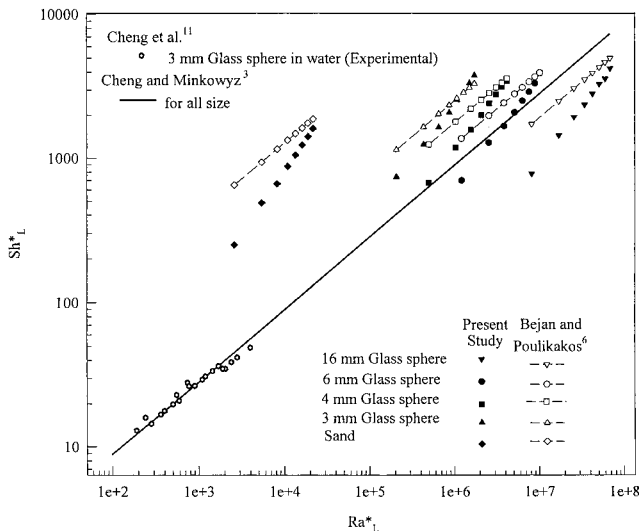


Figure 5. Comparison of experimental mass-transfer data with models due to Cheng and Minkowycz³ and Bejan and Poulikakos⁶ and experiments of Cheng et al.¹¹

This establishes the reliability of the technique and the correlation for physicochemical properties. In the same plot, data for various packings do not fall on one curve exhibiting the effect of packing material on natural convective mass transfer. As the particle size increases, the average Sherwood number approaches the values for a free solution.

The average Sherwood number calculated using effective diffusivity (Sh_L^*) is plotted against the modified Rayleigh number (Ra_L^*) in Figure 5. The experimental data for different packing particles form straight lines of approximately the same slopes. Sh_L^* decreases with increasing particle size for a given Ra_L^* . Cheng and Minkowycz³ modeled heat transfer in porous media assuming Darcian flow. An analogous mass-transfer equation for constant surface concentration is written as

$$Sh_L^* = 0.888(Ra_L^*)^{0.5} \quad (5)$$

This equation represents a single straight line in Figure 5, which does not agree with the experimental values. This indicates the presence of some non-Darcian effects in the present experiments. However, the experimental data of Cheng et al.¹¹ for heat transfer from a vertical plate embedded in a bed of 3-mm glass spheres saturated water match with this model. In their work, Ra_L^* was less than 5000. As discussed in subsequent paragraphs, the non-Darcian effects are not pronounced for lower values of Ra_L^* . It is interesting to note that extrapolated values for 3-mm particle size from the present experiments match their data.

Bejan and Poulikakos⁶ proposed a model based on Forchheimer's equation. They have suggested a nondimensional group (G) as an indicator of the departure from Darcy's flow model. For mass transfer G can be written as

$$G = \frac{\nu}{K} \left[bg \left(\frac{\rho}{\rho_0} - 1 \right) \right]^{-0.5} = \left(\frac{\nu L}{b K D_e Ra_L^*} \right)^{0.5} \quad (6)$$

where b is the Forchheimer's constant that can be given as

$$b = c_F K^{-0.5} \quad (7)$$

Dimensionless form drag constant c_F is believed to have a universal value² of 0.55. As G approaches zero, non-Darcian effects become significant. It can be concluded from eq 6 that, for smaller Ra_L^* , G becomes large. Experimental data of Cheng et al.¹¹ are at low Ra_L^* and thus agree with Darcy's model. For a given system and bulk concentration, G depends on the particle size. Linear regression of the data reveals the following dependence of G on d_p with $R^2 = 99.6\%$:

$$G = 27.77 [d_p \text{ (mm)}]^{-1.54} \quad (8)$$

For bigger particles non-Darcian effects are significant. Bejan and Poulikakos⁶ concluded that the local heat-transfer coefficient is related to Ra_∞ , the large-Reynolds-number Rayleigh number. For mass transfer Ra_∞ can be given as

$$Ra_\infty = \frac{gL^2(\rho/\rho_0 - 1)}{bD_e^2} = Ra_L^* \frac{L}{bD_e K} \quad (9)$$

The average Sherwood number thus can be related as Ra_L^* :

$$Sh_L^* = 0.988(Ra_\infty)^{0.25} \quad (10)$$

As is evident from Figure 5, estimated values are close to the experimental ones only at larger embedded lengths. For shorter lengths the model deviates significantly. This could be due to the exclusion of inertia effects in the model.

Hong et al.¹⁸ included non-Darcian effects such as inertia and a boundary layer adjacent to the surface and proposed parameter ξ as an indicator of departure from Darcian flow:

$$\xi = \frac{2}{Gr_L^{0.5} Da_L} \quad (11)$$

A very large value of ξ indicates that non-Darcian effects

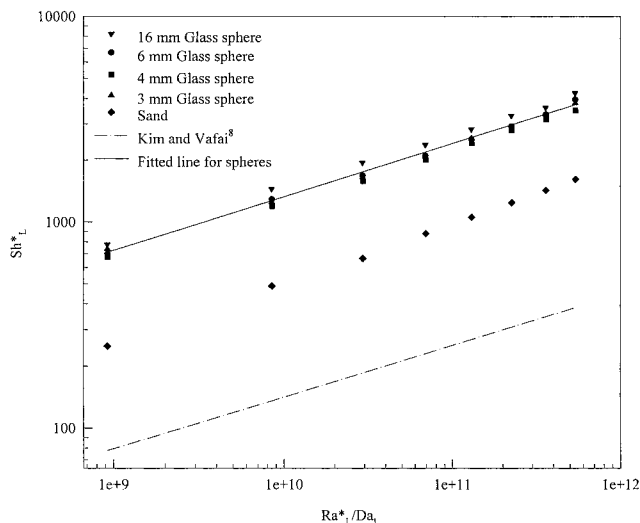


Figure 6. Comparison of experimental mass-transfer data with the model of Kim and Vafai.¹⁰

are not significant. For this model, the local Sherwood number can be written as

$$Sh_x^* = -(0.25 Gr_x)^{1/4} (\theta_0'(0) + \xi \theta_1'(0) + \xi^2 \theta_2'(0) + \xi^3 \theta_3'(0)) \quad (12)$$

The values of $\theta_i'(0)$ depend on Sc (or Pr) and are given for $Pr = 5.4$ and 0.72 in the reference. When $\xi \rightarrow \infty$, eq 14 reduces to Cheng and Minkowycz's eq 5. Because Schmidt numbers are high in the present work, this model was not compared.

Kim and Vafai⁸ used Brinkman-extended Darcy's flow model to predict heat-transfer coefficients. For the condition $Ra_L^* \ll Da_L^{-0.05}$, which is satisfied for the present system, the average mass-transfer coefficient can be obtained from

$$Sh_L^* = 0.785 \left(\frac{Ra_L^*}{Da_L} \right)^{0.25} \quad (13)$$

The experimental values of Sh_L^* are plotted against Ra_L^*/Da_L in Figure 6 with eq 13. It can be observed that the model underestimates Sh_L^* . All data points, except those for sand, seem to fall on a single straight line parallel to the model equation. The nonconfirming behavior of sand is attributed to the irregular shape and size of the sand particles, which lead to a tortuosity factor different from 4. Results for spherical glass particles are fitted into a straight line represented by the following equation with $R^2 = 98.4\%$:

$$Sh_L^* = 3.32 \left(\frac{Ra_L^*}{Da_L} \right)^{0.26} \quad (14)$$

5. Conclusion

Mass-transfer coefficients from vertical surfaces embedded in a variety of packing materials saturated with a cupric sulfate solution were obtained experimentally using LDCT. Average Sherwood numbers were calculated, and data were compared with several mathematical models and other experiments available in the literature. Models based on simple Darcy's flow fail to

predict mass-transfer coefficients in general. Inclusion of non-Darcian effects in the model brings the predicted data closer to the experiments. A model due to Bejan and Poulikakos⁶ using Forchheimer's equation is found to be close only for larger embedded lengths. Kim and Vafai's¹⁰ model, which is based on Brinkman-extended Darcy's flow model, with a corrected constant, predicts very closely for spherical particles. Average Sherwood numbers can be obtained from eq 14 for surfaces embedded in spherical particles.

Acknowledgment is due to King Fahd University of Petroleum & Minerals for use of their facilities.

Nomenclature

- A = mass-transfer area, cm^2
- b = Forchheimer's constant (eq 7)
- C_{acid} = bulk concentration of acid, mol/L
- C_b = bulk concentration of cupric sulfate, mol/L
- c_F = dimensionless drag constant
- D = molecular diffusivity, cm^2/s
- Da_L = Darcy's number, $k/\epsilon L^2$.
- D_e = effective diffusivity, eq 2, cm^2/sec .
- d_p = particle diameter, mm
- F = Faraday's constant
- g = acceleration due to gravity, cm/s^2
- G = parameter defined in eq 8
- Gr_L = average Grashof number, $gL^3(\rho/\rho_0 - 1)v^2$
- I_L = limiting current, mA
- K = permeability (eq 3)
- k_L = average mass-transfer coefficient, cm/s
- L = embedded length of the sample, cm
- Pr = Prandtl number
- Ra_L = average Rayleigh number, $Sc \times Gr_L$.
- Ra_L^* = average modified Rayleigh number, $gKL(\rho/\rho_0 - 1)/vD_e$.
- Ra_∞ = large-Reynolds-number Rayleigh number (eq 9)
- Sc = Schmidt number
- Sh_L = average Sherwood number estimated with molecular diffusivity, $k_L L/D$
- Sh_L^* = average Sherwood number estimated with effective diffusivity, $k_L L/D_e$.
- T = temperature, $^\circ\text{C}$
- z = number of electrons in a reduction reaction

Greek Letters

- ϵ = porosity
- ν = kinematic viscosity, cm^2/s
- $\theta_i'(0)$ = constants defined in ref 18
- ξ = parameter defined in eq 11
- μ = viscosity, P
- ρ = bulk density of the solution, g/cm^3
- ρ_0 = density of the solution at the surface, g/cm^3
- τ = tortuosity factor

Appendix

Correlations for physicochemical properties of acidic cupric sulfate solutions:

$$\rho \text{ (g/cm}^3\text{)} = 0.999448 + 0.14807 C_b + 0.060816 C_{\text{Acid}} - 4.246 \times 10^{-4} \Delta T + 0.00151 (C_b)^2 - 7.043 \times 10^{-4} (C_{\text{Acid}})^2 - 4.47 \times 10^{-6} \Delta T^2 - 0.00456 C_b C_{\text{Acid}} - 6.0 \times 10^{-5} C_b \Delta T + 1.81 \times 10^{-5} C_{\text{Acid}} \Delta T$$

$$\mu \text{ (P)} = 0.01[0.89954 + 0.4537 C_b + 0.14063 C_{\text{Acid}} - 0.019235 \Delta T + 0.232 (C_b)^2 + 0.02894 (C_{\text{Acid}})^2 + 0.000321 \Delta T^2 + 0.09496 C_b C_{\text{Acid}} - 0.01504 C_b \Delta T - 0.004953 C_{\text{Acid}} \Delta T]$$

$$D \text{ (cm}^2\text{/s)} = ((T + 273.15)/\mu)(1.98 + 2.34 C_b) \times 10^{-10}$$

Here, $\Delta T = T - 25^\circ\text{C}$.

Literature Cited

- (1) Lage, J. L. The Fundamental Theory of Flow through Permeable Media from Darcy to Turbulence. In *Transport Phenomena in Porous Media*; Ingham, D. B., Pop, I., Eds.; Pergamon: Oxford, U.K., 1998.
- (2) Nield, D. A.; Bejan, A. *Convection in Porous Media*, 2nd ed.; Springer-Verlag: New York, 1999.
- (3) Cheng, P.; Minkowycz, W. J. Free Convection about a Vertical Flat Plate Embedded in a Porous Medium with Application to Heat Transfer from a Dike. *J. Geophys. Res.* **1977**, *82* (14), 2040.
- (4) Cheng, P.; Hsu, C. T. High-order Approximations for Darcian Free Convective Flow about a Semi-infinite Vertical Flat Plate. *Trans. ASME: J. Heat Transfer* **1984**, *106*, 143.
- (5) Joshi, Y.; Gebhart, B. Vertical Natural Convection Flows in Porous Media Calculations of Improved Accuracy. *Int. J. Heat Mass Transfer* **1984**, *27* (1), 69.
- (6) Bejan, A.; Poulikakos, D. The Non-Darcy Regime for Vertical Boundary Layer Natural Convection in a Porous Medium. *Int. J. Heat Mass Transfer* **1984**, *27* (5), 717.
- (7) Plumb, O. A.; Huenefeld, J. C. Non-Darcy Natural Convection from Heated Surfaces in Saturated Porous Media. *Int. J. Heat Mass Transfer* **1981**, *24* (4), 765.
- (8) Hsu, C. T.; Cheng, P. The Brinkman Model for Natural Convection about a Semi-infinite Vertical Flat Plate in a Porous Medium. *Int. J. Heat Mass Transfer* **1985**, *28* (3), 683.
- (9) Evans, G. H.; Plumb, O. A. Natural Convection from a Vertical Isothermal Surface Embedded in a Saturated Porous Medium. *AIAA-ASME Thermophysics and Heat Transfer Conference*, Palo Alto, CA, 1978; Paper 78-HT-55.
- (10) Kim, S. J.; Vafai, K. Analysis of Natural Convection about a Vertical Plate Embedded in Porous Medium. *Int. J. Heat Mass Transfer* **1989**, *32* (4), 665.
- (11) Cheng, P.; Ali, C. L.; Verma, A. K. An Experimental Study of Non-Darcian Effects in a Saturated Porous Medium. *Lett. Heat Mass Transfer* **1981**, *8*, 261.
- (12) Kaviany, M.; Mittal, M. Natural Convection Heat Transfer from a Vertical Plate to High Permeability Porous Media: An Experiment and Approximate Solution. *Int. J. Heat Mass Transfer* **1987**, *30* (5), 967.
- (13) Kaviany, M.; Mittal, M. An Experimental Study of Vertical Plate Natural Convection in Porous Media. In *Heat Transfer in Porous Media and Particulate Flow*; Yao, L. S., Ed.; American Society of Mechanical Engineers: Fairfield, NJ, 1985; pp 175-179.
- (14) Selman, J. R.; Tobais, C. W. Mass-transfer Measurements by the Limiting Current Technique. *Adv. Chem. Eng.* **1981**, *10*, 211.
- (15) Chiang, H. D.; Goldstein, R. J. Application of the Electrochemical Mass Transfer Technique to the Study of Buoyancy-driven Flows. In *Transport Phenomena in Heat and Mass Transfer*; Reizes, J. A. Ed.; Proceedings of the Fourth International Symposium on Transport Phenomena in Heat and Mass Transfer, Sydney, 1991; Elsevier: New York, 1991; Vol. 1, p 1.
- (16) Smith, J. M. *Chemical Engineering Kinetics*; McGraw-Hill International Book Company: New York, 1981.
- (17) Skelland, A. H. P. *Diffusional Mass Transfer*; R.E. Krieger Publishing Company: Malabar, FL, 1985.
- (18) Hong, J. T.; Tien, C. L.; Kaviany, M. Non-Darcian Effects on Vertical-plate Natural Convection in Porous Media with High Porosities. *Int. J. Heat Mass Transfer* **1985**, *28* (11), 2149.

Received for review May 24, 1999

Revised manuscript received October 14, 1999

Accepted October 19, 1999

IE990357F